Ice Island and Iceberg Fluxes from Canadian High Arctic Sources

Prepared for the
Innovation Policy Group
of
Transport Canada

By

The Water and Ice Research Laboratory
Department of Geography and Environmental Studies
Carleton University

and

Laboratory for Cryospheric Research
Department of Geography
University of Ottawa

October 2013

Ice Island and Iceberg Fluxes from Canadian High Arctic Sources

Derek Mueller and Anna Crawford
The Water and Ice Research Laboratory
Department of Geography and Environmental Studies
Carleton University

Luke Copland and Wesley Van Wychen
Laboratory for Cryospheric Research
Department of Geography
University of Ottawa

October 2013

This report reflects the views of the authors (or the performing organization) and not necessarily those of Transport Canada.

Project Team

D.R. Mueller, Project Leader
L. Copland, Project Leader
W. Van Wychen, PhD Candidate
A. Crawford, PhD Candidate

Un sommaire français se trouve avant la table des matières.

ACKNOWLEDGEMENTS

Imagery for this project was obtained through Natural Resources Canada, the Canadian Ice Service, the Canadian Space Agency's SOAR and SOAR-E programs and the Alaska Satellite Facility. Cindy Lopes, Gregory Lewis-Paley and Laura Derksen are acknowledged for their assistance in preparing imagery.

EXECUTIVE SUMMARY

This project was initiated by the Northern Transportation Adaptation Initiative with the aim of quantifying the production rates of ice islands and icebergs in the Canadian High Arctic. A first step toward understanding the risk that these ice hazards pose to vessels transiting through the Canadian Arctic (e.g. Baffin Bay, the Northwest Passage and Beaufort Sea) is to estimate the fluxes from their source areas. These drifting ice hazards have been observed throughout the Canadian Arctic in recent years (Derksen et al. 2012; Peterson 2011) and are poised to become a greater threat due to the projected increase of transportation in the Arctic (Stephenson et al. 2013). It is thus necessary to understand the production rates and thicknesses of ice islands and icebergs to quantify their regional fluxes. This was undertaken through analyses of ice island and iceberg sources in the Canadian Arctic.

Ice islands are large tabular icebergs which originate from the ice shelves of northern Ellesmere Island and historically have had surface areas up to 1,030 km^2 (Koenig et al. 1952). The original 'Ellesmere Ice Shelf' was estimated to have an areal extent of 8,900 km^2 in the early 20^{th} century (Vincent et al. 2001). Since then, decreases in its areal extent due to ice shelf break-up (calving) events have created numerous ice islands. These ice islands have been known to drift in the Beaufort Gyre for several decades, making them potential hazards to offshore industry or vessels operating in the Western Canadian Arctic for long periods of time. Ice islands also pose as hazards in the Eastern Canadian Arctic - normally originating from Northwest Greenland (e.g., the Petermann and Ryder glaciers) and following a common drift route through Baffin Bay and the Labrador Sea (Peterson 2011; L. Desjardins pers. comm.).

The ice island flux from the Ellesmere Island ice shelves was calculated from records of areal extent loss and ice shelf thickness. The areal extent of the Ellesmere Island ice shelves was monitored in geographic information system (GIS) software. The Ellesmere Island coastline and the 1998 ice shelves' extents were acquired through the National Topographic Database (NTDB). Regional synthetic aperture radar (SAR) imagery was acquired between 1998 and 2012, projected in GIS and overlain on the original NTDB coastline layer. The areal extents of the ice shelves were determined by digitizing the perimeter of each ice shelf, which appears brighter than surrounding sea ice in SAR imagery. The difference in areal extent between images indicates ice shelf calving, a by-product of which is the creation of drifting ice islands. Ice

penetrating radar thickness measurements were recorded from a selection of the Ellesmere Island ice shelves and range from 15 m (Peterson Ice Shelf, White (2012)) to 94 m (Milne Ice Shelf, Mortimer et al. (2012)), with a representative value of 41 ±6 m used for all thickness calculations in this analysis. Ice island flux was calculated by multiplying the ice shelf areal loss over time by this thickness. The associated mass was determined by multiplying the volume by an ice density value of 890 kg m^{-3} (Jeffries et al. 1991).

Since 1998, the northern coast of Ellesmere Island has lost a total of 552 km^2 of ice shelf extent (Figure 3). A large amount of this loss is related to calving events which occurred between 2002 and 2008 from the Ayles, Petersen (Copland et al. 2007), Wootton (Pope et al. 2012), Serson, Markham and Ward Hunt ice shelves (Mueller et al. 2003; Mueller et al. 2008). Calving events have continued in recent years (White 2012; Derksen et al. 2012). This has likely provided the source of hundreds of drifting ice islands in the Arctic Ocean, some of which have been observed in the Beaufort Sea, the Canadian Arctic Archipelago (CAA) and the Northwest Passage. These events equate to an estimate of 20 gigatons (Gt) of ice shelf mass lost to ice island calvings since 2001. There is a large range of annual flux rates (Gt a^{-1}) due to the sporadic nature of calving events, with minimum and maximum fluxes of 0 and 11 Gt a^{-1}, respectively. The maximum flux was observed in 2008 which corresponds to a major break-up event involving the Ward Hunt, Serson and Markham ice shelves (Mueller et al. 2008).

To determine the iceberg flux from glacier and ice cap sources in the CAA, the surface velocities of the main glaciers which terminate in the ocean were calculated and multiplied by their terminal thickness. Velocity maps were created from pairs of Radarsat-2 satellite imagery processed using a speckle tracking algorithm. Topographic effects were removed with the use of a digital elevation model, and the velocities determined over the 24 days between Radarsat-2 acquisitions were standardized to yearly values. Glacial ice thickness data was acquired primarily from previous airborne radio-echo sounding measurements made by NASA (2012), Dowdeswell et al. (2004), Gogenini (1995) and Narod et al. (1988).

Surface ice velocities in the Queen Elisabeth Islands (QEI) on large tidewater-terminating outlet glaciers are generally >100 m a^{-1}. Total ice discharge via calving from the QEI is currently estimated to be between 1.5 and 4.0 Gt a^{-1}. The Prince of Wales Icefield provides the largest single contributor to mass loss via calving, with approximately half of total ice loss coming from

just two glaciers: Trinity and Wykeham. The other glaciers, ice caps and icefields in the QEI (e.g. Northern Ellesmere Ice Cap, Manson Icefield, Sydkap Ice Cap) are relatively minor contributors to iceberg fluxes at the present day. However, the frequent occurrence of surge-type glaciers on these ice caps suggests that iceberg discharges may vary by an order of magnitude or more between years. Due to the lack of knowledge with regard to the length of surge cycles for many glaciers within the QEI, future predictions of mass loss from the region are difficult. This necessitates the continual monitoring of surface velocities for these ice masses to produce year-to-year updates for iceberg production rates.

Overall, this study provides one of the first reports of annual ice island and iceberg fluxes for the Canadian High Arctic. There is large inter-annual variation, ranging from 1.6 to 13.3 Gt a^{-1}, due to the irregular nature of calving events from ice shelves and surging from tidewater terminating glaciers. The average ice island flux of the Ellesmere Island ice shelves over the period from 1998 to 2012 was 1.8 Gt a^{-1}, providing a primary source of hazards for shipping activity in the Western Canadian Arctic. The 2012 iceberg flux from CAA glaciers was estimated at 1.5 to 4.0 Gt, with these icebergs providing potential hazards to Eastern Canadian Arctic operations. This research provides information for use by the marine transportation industry on the production and occurrence of ice hazards. It is recommended that monitoring and analysis of calving events and glacial surge velocities continue. This will aid in ice hazard risk surveillance, assessment and management planning in industrially active Canadian waters.

SOMMAIRE

Ce projet a été lancé dans le cadre de l'Initiative d'adaptation des transports dans le Nord dans le but de mesurer le taux de production d'îles de glace et d'icebergs dans le Haut-Arctique canadien. Pour mieux comprendre le risque que posent ces formations de glace périlleuses pour les navires qui passent par l'Arctique canadien (p. ex. la baie de Baffin, le Passage du Nord-Ouest et la mer de Beaufort), il faut d'abord évaluer les flux dans les endroits où ces formations prennent naissance. Au cours des dernières années, ces formations de glace dangereuses ont été aperçues un peu partout dans l'Arctique canadien (Derksen et coll. 2012; Peterson 2011) et sont en passe de présenter un danger encore plus important en raison de l'augmentation prévue du transport dans l'Arctique (Stephenson et coll. 2013). Il faut donc mieux comprendre les taux de production et l'épaisseur des îles de glace et des icebergs afin de mesurer leur flux régional. Ce travail a été entrepris grâce à l'analyse des sources d'îles de glace et d'icebergs dans l'Arctique canadien.

Les îles de glace sont de gros icebergs plats qui proviennent des plateformes de glace du nord de l'île d'Ellesmere. Historiquement, leur superficie peut mesurer jusqu'à 1 030 km^2 (Koenig et coll. 1952). On estime que la « plateforme de glace d'Ellesmere » originale occupait un territoire de 8 900 km^2 au début du 20^e siècle (Vincent et coll. 2001). Depuis ce temps, la diminution de sa superficie, attribuable à des épisodes de morcellement de la plateforme de glace (vêlage), a entraîné la formation de nombreuses îles de glace. Il est connu que ces îles de glace peuvent dériver dans le tourbillon de Beaufort pendant plusieurs dizaines d'années, ce qui pose un danger persistant pour les industries extracôtières et les navires dans l'ouest de l'Arctique canadien. Les îles de glace présentent aussi un danger dans l'est de l'Arctique canadien. Elles proviennent souvent du nord-ouest du Groenland (notamment des glaciers Petermann et Ryder) et suivent le même chemin de dérive en passant par la baie de Baffin et la mer du Labrador (Peterson 2011; L. Desjardins comm. pers.).

On a calculé le flux des îles de glace provenant des plateformes de glace de l'île d'Ellesmere à partir de données sur la superficie perdue et sur l'épaisseur des plateformes de glace. L'étendue des plateformes de glace de l'île d'Ellesmere a été surveillée à l'aide d'un système d'information géographique (SIG). En 1998, l'étendue de la côte de l'île d'Ellesmere et de ses plateformes de glace a été enregistrée dans la Base nationale de données topographiques (BNDT). De 1998 à

2012, on a pris des images de radar à synthèse d'ouverture (RSO), puis on les a projetées dans un SIG et superposées au tracé original de la côte qui se trouvait dans la BNDT. La superficie des plateformes de glace a été déterminée grâce à la numérisation du périmètre de chaque plateforme, qui paraît plus claire que la glace de mer environnante dans les images captées par RSO. La différence de superficie entre les images révèle le taux de vêlage des plateformes de glace, qui crée comme sous-produit des îles de glace dérivantes. Des mesures de l'épaisseur de la glace réalisées avec un radar d'épaisseur de glace ont été consignées à partir d'une sélection de plateformes de glace dans l'île d'Ellesmere. L'épaisseur varie, allant de 15 m (plateforme Peterson, White [2012]) à 94 m (plateforme de Milne, Mortimer et coll. [2012]). Une valeur représentative de 41 ±6 m a été utilisée pour tous les calculs d'épaisseur dans cette analyse. On a calculé le flux des îles de glace en multipliant la perte de superficie des plateformes de glace avec le temps par la valeur représentative de l'épaisseur. On a calculé la masse en multipliant le volume par une valeur de densité de glace de 890 kg/m^3 (Jeffries et coll. 1991).

Depuis 1998, la rive nord de l'île d'Ellesmere a perdu au total 552 km^2 de ses plateformes de glace (Figure 3). Cette perte est attribuable en grande partie à des épisodes de vêlage, qui se sont produits de 2002 à 2008 sur les plateformes Ayles, Petersen (Copland et coll. 2007), Wootton (Pope et coll. 2012), Serson, Markham et Ward Hunt (Mueller et coll. 2003; Mueller et coll. 2008). Le vêlage s'est poursuivi au cours des dernières années (White 2012; Derksen et coll. 2012). Cette activité a probablement donné lieu à des centaines d'îles de glace dérivantes dans l'océan Arctique, certaines ayant été aperçues dans la mer de Beaufort, dans l'archipel arctique canadien et dans le Passage du Nord-Ouest. La production d'îles de glace par vêlage a entraîné la perte d'environ 20 gigatonnes (Gt) de plateforme de glace depuis 2001. Les taux de flux annuels (Gt a^{-1}) varient beaucoup à cause de la nature sporadique des épisodes de vêlage, les flux minimum et maximum étant respectivement de 0 et de 11 Gt a^{-1}. Le flux maximum a eu lieu en 2008, année où un épisode majeur a morcelé une partie des plateformes de glace Ward Hunt, Serson et Markham (Mueller et coll. 2008).

Pour déterminer le flux des icebergs provenant de glaciers et de calottes glacières dans l'archipel arctique canadien, on a calculé la vitesse superficielle des principaux glaciers qui bordent l'océan et on l'a multipliée par l'épaisseur du glacier là où il se déverse dans l'océan. Des cartes de vitesse ont été créées à partir de paires d'images provenant du satellite Radarsat-2,

traitées à l'aide d'un algorithme de suivi du chatoiement. On a éliminé les effets topographiques à l'aide d'un modèle altimétrique numérique, et les vitesses établies pendant la période de 24 jours qui séparait chaque extraction de données du satellite Radarsat-2 ont été normalisées pour en faire des valeurs annuelles. Les données sur l'épaisseur des glaciers provenaient surtout de mesures aériennes par échos radars réalisées auparavant par la NASA (2012), Dowdeswell et coll. (2004), Gogenini (1995) et Narod et coll. (1988).

Dans les îles de la Reine-Élisabeth, la vitesse superficielle des grands glaciers qui se jettent dans l'eau de marée est généralement supérieure à 100 m a^{-1}. On estime que le débit de glace produit par vêlage dans les îles de la Reine-Élisabeth se situe actuellement entre 1,5 et 4,0 Gt a^{-1}. Parmi les contributeurs uniques à la perte de masse par vêlage, le champ de glace Prince-de-Galles est le plus important, et environ la moitié de la glace perdue provient de deux glaciers en particulier : Trinity et Wykeham. À l'heure actuelle, les autres glaciers, calottes glacières et champs de glace dans les îles de la Reine-Élisabeth (p. ex., la calotte glaciaire du nord de l'île d'Ellesmere, le champ de glace Manson et la calotte glaciaire Sydkap) jouent un rôle relativement mineur dans le flux des icebergs. Cependant, la fréquence élevée de production de glaciers en crue dans ces calottes glaciaires donne à penser que la production d'icebergs peut varier d'un ordre de grandeur ou plus d'une année à l'autre. À cause du manque de données sur la durée des cycles de crue des icebergs pour de nombreux glaciers dans les îles de la Reine-Élisabeth, il est difficile de prédire les pertes de masse glaciaire dans la région. Il faut exercer une surveillance constante de la vitesse superficielle de ces masses de glace afin de pouvoir mettre à jour les taux de production d'icebergs chaque année.

Dans l'ensemble, cette étude offre l'un des premiers rapports sur les flux annuels d'îles de glace et d'icebergs dans le Haut-Arctique canadien. Ce flux varie beaucoup sur plusieurs années et peut aller de 1,6 à 13,3 Gt a^{-1}, en raison de la nature irrégulière des épisodes de vêlage à partir des plateformes de glace et des crues à partir de glaciers qui se déversent dans l'eau de marée. Le flux moyen des îles de glace issues des plateformes de glace de l'île d'Ellesmere de 1998 à 2012 était de 1,8 Gt a^{-1}, ce qui a constitué un danger important pour le transport maritime dans l'ouest de l'Arctique canadien. On a estimé que le flux d'icebergs provenant en 2012 des glaciers de l'archipel arctique canadien a totalisé entre 1,5 et 4,0 Gt. Ces icebergs présentaient un risque pour les activités dans la partie est de l'Arctique canadien. Ces travaux de recherche constituent de

l'information utile sur la production et l'occurrence des dangers dus aux glaces pour l'industrie du transport maritime. On recommande de poursuivre la surveillance et l'analyse des épisodes de vêlage et de la vitesse de crue des glaces. Dans les eaux canadiennes où des industries exercent leurs activités, ces travaux aideront à planifier la surveillance, l'évaluation et la gestion des dangers dus aux glaces.

TABLE OF CONTENTS

LIST OF FIGURES

LIST OF TABLES

LIST OF SYMBOLS AND ABBREVIATIONS

Symbols

m	meter
m a^{-1}	meters per annum
Gt	gigatons
Gt a^{-1}	gigatons per annum

ASTER	Advanced Spaceborne Thermal Emission and Reflection Radiometer
CAA	Canadian Arctic Archipelago
GIS	Geographic information system
IPR	Ice penetrating radar
MODIS	Moderate Resolution Imaging Spectroradiometer
NTDB	National Topographic Database
ROI	Region of interest
SAR	Synthetic aperture radar
QEI	Queen Elizabeth Islands

1 Introduction

This project aims to quantify the production rates of ice islands and icebergs in the Canadian High Arctic. These drifting ice hazards have become more prevalent in recent years due to the breakup of features such as ice shelves. They are poised to become more of a threat to vessels (Figure 1) in the Canadian Arctic due to the observed (Pizzolato et al. 2013) and projected (Stephenson et al. 2013) increase of transportation in the region. Baseline information on the number and distribution of ice islands and icebergs present in Canadian waters, and characteristics of their sources, is currently very limited. A first step toward understanding the risk that these ice hazards pose is to estimate their fluxes from their source areas. This document reports on the fluxes of ice islands from the Canadian Arctic ice shelves along the northern coast of Ellesmere Island and the flux of icebergs at tidewater glaciers at the margins of the Queen Elizabeth Islands (QEI).

2 Part A – Ice Islands:

2.1 Background

Arctic ice islands were discovered by American military and Soviet scientists independently in the late 1940s north of the Beaufort and Chukchi seas (Fletcher 1950; Belkin and Kessel 2011). These masses of floating ice, described as large, tabular icebergs (MANICE 2005), were typically on the order of several kilometers long and up to 1,030 km^2 in areal extent (Koenig et al. 1952). They were viewed as a military asset during the Cold War since planes could land on these mobile platforms in the remote Arctic Basin (Althoff 2007). Shortly after the discovery of ice islands, it was proposed that the ice shelves along the northern coast of Ellesmere Island provided their source, and glaciological investigations were launched to study this unique phenomenon (Hattersley-Smith et al. 1955). It is clear from the anecdotal evidence in the late 19^{th} and early 20^{th} century journals of explorers such as Lt. Pelham Aldrich of the British Royal Navy and Cmdr. Robert Peary of the US Navy, that the 'Ellesmere Ice Shelf' (unofficial name) was far more extensive in the past, possibly comprising an area of up to 8,900 km^2 at the start of the 20^{th} century (Vincent et al. 2001). A period of rapid ice shelf loss followed, which coincided with several decades of pronounced regional warming, in the 1930s and 40s. By the time the ice

shelves were mapped in 1959, they were reduced to ~2,300 km^2 and over the next decade they were further reduced by approximately 1,700 km^2 (Hattersley-Smith 1967; Jeffries 1986, 1992). The climate cooled somewhat in the 1970s and 1980s and the only major changes that occurred during that time were observed in the early 1980s when the Ward Hunt Ice Shelf calved twice (Jeffries 1982; Jeffries and Serson 1983).

At that time, calving events along the coast of Ellesmere Island provoked concern related to risks to Arctic infrastructure. Surveys along the northern coast of mainland NWT, Yukon and Alaska revealed a substantial number of ice islands and smaller fragments (Barton et al. 1972; Spedding 1974, 1977). Ice islands have been known to drift in the Beaufort Gyre for up to several decades, so these ice hazards were likely remnants of earlier ice shelf calving events (Figure 2). Dome Petroleum funded research in the 1980s on Canadian ice shelves and ice islands since they had plans to drill in the Beaufort Sea and needed to assess the risk to their operations. This line of inquiry was dropped when the price of oil fell, making Arctic oil uneconomic to develop. A relative lull in resource exploration and ice shelf/ice island research followed until the early 2000s, with the exception of Hobson's Choice Ice Island, that was occupied as a research base for several seasons before drifting into the Canadian Arctic Archipelago (CAA) and breaking up (Hobson 1989). Ice islands also pose as hazards in the Eastern Canadian Arctic - normally originating from Northwest Greenland (e.g. the Petermann and Ryder glaciers) and following a common drift route through Baffin Bay and the Labrador Sea (Peterson 2011; L. Desjardins pers. comm.). In this report, the ice shelf calving over the period from 1998 to present (2012) will be determined to enable calculation of an ice island flux from the northern coast of Ellesmere Island, the Canadian source of ice islands which then drift through the Western Canadian Arctic region. This will allow for a prediction of ice hazard occurrence in industrially active Canadian waters.

2.2 Methods

2.2.1 Determination of ice shelf extents

This project made extensive use of Geographic Information System (GIS) software (ArcMap 10.1, ESRI, Redlands, CA) to conduct spatial analysis. National Topographic Database (NTDB) geospatial data at 1:250,000 scale was acquired through Geogratis (geogratis.cgdi.gc.ca). This consisted of the coastline and glacier outlines from map sheets in National Topographic Service zones 560, 340 and 120. These polygons were merged to form continuous geospatial layers and then projected to a custom Albers equal area projection centred on the northern Ellesmere Island region. These maps were produced by Natural Resources Canada in May 2009 from data sources including aerial stereo photographs from 1959, Landsat imagery south of ~82^{o}N and Radarsat-1 imagery in 2004. This dataset is considered to have a horizontal accuracy on the order of 60 m. These products do not consider ice shelves at all and the glacier outlines were found to be out of date.

The areas where ice shelves were marked on the 1959/1960 maps were outlined with polygons in the GIS. These regions of interest (ROIs) were used to query a custom-built spatial database (using open source software PostgreSQL 9.2 and PostGIS 2.0). An archive of synthetic aperture radar (SAR) imagery was produced using custom-built python scripts to open individual imagery and store image metadata in the spatial database. The database was then queried to determine which images contained or intersected with the ice shelf ROIs from 1998 to 2012. These candidate images were then filtered to select a subset of images (Table A-1) that most efficiently covered the ice shelves and yet respected the following. Ultimately the images that were preferentially used were the highest resolution available and they were acquired as close as possible to January 1 of every year. Mid-winter imagery is desirable since the contrast between ice types is maximal when liquid water is not present in the snow (Figure 3). When imagery containing the ROI was not available, coverage was provided (partly or completely) using imagery that intersected with the ROIs. Other imagery was used to aid in the interpretation of ice types, including MODIS, ASTER and Formosat-2 imagery.

Candidate imagery was extracted using custom-built python scripts or MapReady 3.1 (Alaska Satellite Facility) to convert the data into an amplitude detected image that was byte-scaled and stretched to a 2 sigma level for maximum contrast. Regions of high backscatter appear brighter (due to various surface and volume scattering mechanisms), whereas darker regions denote low radar return due to specular reflection or attenuation of the microwave radiation by the surface. As is typical with SAR imagery, image artifacts related to the viewing geometry of side-looking radar (foreshortening, layover and shadow) were ignored. The imagery was projected to the Albers equal area projection and compared to the coastline layer, described above. In about half the images the geolocation was misaligned by up to several hundred metres. This was corrected by shifting the image, as required, to align it with an overall best fit to the coastline. In some cases there was a residual error in geolocation on the order of 100 m in certain regions of the image. This can be ignored at the scale used in this study as minor misalignment does not influence ice area calculations.

Each ice shelf was digitized for each year under study from the available SAR imagery. In most cases, the coastline was exploited as a natural boundary for the ice shelf, leaving only the calving fronts to be digitized. The uncertainty in the ice shelf area depends primarily on the image resolution, and was calculated using the equivalent square method (Ghilani 2000).

2.2.2 Ice thickness

There are only a few reliable measurements of recent ice shelf thickness in the Canadian Arctic. Part of the reason for this is the logistical difficulty of operating in this remote region. However, it is also partly due to the relatively high salinity of certain ice types that comprise the ice shelves. The standard technique for measuring ice thickness is to use ice (ground) penetrating radar (IPR). This method works by pulsing radio waves through the ice to the bottom ice/water interface where it reflects the signal back to the detector. This reflection is recorded and the time it takes for the return is noted and converted into a distance under the assumption that radio waves travel at 1.70×10^{8} m s^{-1} in cold ice (Mortimer et al., 2012; White 2012).

Extensive ice thickness surveys have been conducted on the Milne and Petersen ice shelves; however there are large tracks of the Petersen Ice Shelf that are too saline to obtain a return (White 2012). Results from the Milne Ice Shelf indicate a mean thickness of 55 m with a

standard deviation of 22 m (Mortimer et al. 2012). The maximum thickness (94 m) was observed near a tributary glacier and there were thicknesses of < 20 m only in specific places near cracks in the ice. The Milne Ice Shelf is likely the thickest of the ice shelves along the northern coast of Ellesmere Island owning to its relatively high glacier influence. The Petersen Ice Shelf had a mean thickness of 29 m with a standard deviation of 24 m (White 2012). Here there were thick areas near tributary glaciers (up to 74 m) and also regions where the ice shelf thickness was smaller (15 m) than would be necessary to satisfy the definition of an Arctic ice shelf. There are also some recent helicopter electromagnetic induction data from the Ward Hunt Ice Shelf which indicate a thickness on the order of 30-40 m (C. Haas, pers. comm.). A single IPR measurement exists for the Ayles Ice Island which was visited in 2007 and had a thickness of 42-45 m (Copland et al. 2007). In sum, there is a high degree of variability in measured ice shelf thickness (Table 1). For the purposes of this report, we calculated a representative thickness of 40.6 m by averaging the thickness of each ice shelf in Table 1. We use the standard error of this mean (5.6 m) to calculate uncertainties in the ice island mass flux.

Table 1. Recorded ice thicknesses of select Ellesmere Island ice shelves (sd = standard deviation).

Ice shelf	Mean thickness (m)	Range in thickness (m)	Number of samples	Source
Petersen	29 (sd: 24)	< 1 m – 106 m	12,746	White 2012
Milne	55 (sd: 22)	< 1 - 94	> 15,000	Mortimer 2012
Ward Hunt	~35	30-40	N/A	Haas, pers. comm.
Ayles	43.5	42-45	2	Copland et al. 2007

2.2.2.1 Flux calculation

Calculation of the ice island flux was conducted by subtracting the areal extent of ice shelves from one year to the next and then multiplying by the presumed thickness. Uncertainty in the change in areal extent was propagated by combining the absolute error in quadrature. The uncertainty in the volume was propagated by combining relative error in quadrature for the areal extent lost and the uncertainty in ice thickness (Taylor 1997). Volume was then converted to mass by using a representative ice density of 890 kg m^{-3} (Jeffries et al. 1991).

2.3 Results and Discussion

The Ellesmere ice shelves began a period of renewed break-up in 2002 when the Ward Hunt Ice Shelf fractured and calved a small number of ice islands (Mueller et al. 2003). This was followed by the loss of the Ayles Ice Shelf in 2005, the calving of the Petersen Ice Shelf (Copland et al. 2007) and the calving of the Wootton Peninsula Ice Shelf (Pope et al. 2012). In 2008, there was a major break-up event involving the Ward Hunt, Serson and Markham ice shelves (Mueller et al. 2008). This was followed by several calving events in recent years (White 2012; Derksen et al. 2012).

Since 1998, the northern coast of Ellesmere Island has lost a total of 552 km^2 of ice shelf extent (Table 2, Figure 4). This likely provides the main source for hundreds of drifting ice islands in the Arctic Ocean, some of which have been observed near Banks Island south of Sachs Harbour (Hochheim et al. 2012), off the Yukon coast (C. Burn, Carleton University, pers. comm..), near Wainwright (Richard Glenn, Arctic Slope Regional Corporation, pers. comm.) and Barrow (M. Drukenmiller, National Snow and Ice Data Centre, pers. comm.) Alaska, and within the CAA and the Northwest Passage (L. Desjardins and D. Stern, pers. comm.).

Table 2. Calving events of northern Ellesmere Island ice shelves since 2002 from the literature. This study found the total ice shelf extent decreased by 552 km^2 between 2002 and 2012, which is 150 km^2 greater than the sum of areal extent losses listed here.

Ice shelf	Year	Area lost (km^2)	Source
Ward Hunt	2002, 2008, 2011	6, 40, 39	Mueller 2003, Derksen et al. 2012, White 2012, Kealey et al. 2011
Ayles	2005	87	Copland et al. 2007
Peterson	2005, 2006-07	12.6, 8	Copland et al. 2007, White 2012, Copland 2009
Wootton	2005	8	Pope et al. 2012
Serson	2008, 2011	120, 32	Mueller et al. 2008, White 2012, Kealey et al. 2012
Markham	2008	50	Mueller et al. 2008

Using a representative thickness of 41 m, the ice island mass flux since 2001 was 20 Gt of ice. This varies considerably from year-to-year since the process of ice shelf break-up and calving is sporadic. The average flux rate is 1.8 Gt per annum (Gt a^{-1}), but this ranges from no loss in five of those years to up to 11 Gt in 2008 (Figure 5). A large portion of the uncertainty in the actual flux rate is primarily due to the assumed error in ice thickness. Since the thickness of the vast majority of the ice that has already calved was never evaluated, it is impractical to confirm whether a thickness of 41 m is representative of these ice islands. Errors in the areal extent of the ice shelf were estimated to be < 2%. It is possible that misidentified ice types constitute a far greater error; however it is difficult to estimate what this error might be. The median flux uncertainty was 14% for the 6 years where an areal extent change was recorded (Figure 5). This is a reasonable value considering the uncertainty associated with areal and volume calculations which were propagated through the flux calculation.

2.4 Conclusions

GIS analysis of SAR imagery was used to determine ice island flux from the Ellesmere Island ice shelves between 1998 and 2012. We estimated 20 ±3 Gt of ice calved from this vicinity over the 15 year study period. A large variation in annual ice island flux occurs due to the sporadic nature of break-up events documented for these ice shelves over the study period. The 552 km^2 of ice islands subsequently created have been observed in locations of current and future offshore exploration and shipping activity, such as the Beaufort and Chukchi seas and the Northwest Passage (Figure 8). It is necessary to continually monitor events occurring at the Ellesmere Island ice shelves and to increase the spatial extent of ice thickness surveys. This will allow for the observation, and perhaps prediction, of ice shelf collapse and greater accuracy in ice hazard mass calculation. The continuation of this research will aid in ice hazard risk surveillance, assessment and management planning in industrially active, Canadian waters.

3 Part B – Icebergs:

3.1 Background

Recent studies indicate rapid recent increases in glacier mass loss from the CAA as a direct result of warmer air temperatures (Gardner et al. 2011; Sharp et al. 2011). As a consequence the Canadian Arctic has become one of the largest contributors to sea level rise outside of the Greenland and Antarctic ice sheets (Gardner et al. 2011). With increasing glacier mass losses from this region, an important question for marine transportation and offshore infrastructure is exactly how these mass losses are occurring. For glaciers which terminate in the ocean, losses can occur primarily through: (1) increased surface melt or (2) increased discharge of icebergs to the ocean. At the moment we know very little about the magnitude of either of these processes in the Canadian Arctic, let alone how they are varying over time. This study addresses this issue by quantifying the iceberg fluxes entering Canadian waters. This is undertaken by analyzing pairs of Radarsat-2 satellite images acquired between January and May 2012 to derive glacier velocities. The velocities of glaciers where they meet the ocean are multiplied by their thicknesses to derive iceberg fluxes from their termini.

Study Site

The glaciated regions of the QEI (Devon, Ellesmere and Axel Heiberg Islands; Figure 6) comprise ~104,000 km^2 of ice. Within the region there has been a strong trend of summer warming since 2005 (compared to the 2000-2004 period) driven by atmospheric circulations that transport heat from the northwest Atlantic to the QEI. This heat transport has led to increased surface melt and a lengthening of the melt season (Sharp et al. 2011; Gardner et al. 2011). Glacier mass balances since 2005 are nearly five times more negative than the 1963-2004 mean (Sharp et al. 2011). Previous studies have indicated that iceberg calving may contribute up to 40% of total ice losses from the region (Burgess et al. 2005; Van Wychen et al. 2012); however, these estimates are limited to only a few locations that have largely estimated ice discharge rates from data prior to 2005.

3.2 Methods:

3.2.1 Creation of velocity maps

Radarsat-2 fine beam (8 m resolution) and ultrafine beam (3 m resolution) satellite imagery acquired between January and May 2012 is used to determine the surface velocities of all major glaciers and ice caps within the QEI (Table A-2). Surface velocities are determined using a speckle tracking algorithm based on that used by Short and Gray (2005). This method uses a cross-correlation algorithm to determine the relative displacement between a pair of Radarsat-2 images, typically acquired in repeat orbits with 24-day separation. Minimal snowfall and/or melt between image acquisitions is required to track surface patterns and allow the ice surface displacements to be measured, so image acquisitions were conducted during mid-winter to late-winter time periods.

Displacement of the ice surface is determined over the entire extent of an image using moving match windows of ~450 x 350 m in size. The 1:250,000 Canadian Digital Elevation Dataset is used to remove topographic effects from the velocity calculations. Ice motion is assumed to be parallel to the ice surface, and is calibrated against known stationary regions such as bedrock outcrops. Velocities are then determined from the calibrated displacement and standardized to annual values. This dataset is manually checked to remove incorrect matches caused when the speckle tracking process finds a stronger correlation with an incorrect pixel than

the true match. This often occurs in rapidly flowing areas and in locations where surface patterns change between satellite image acquisitions (e.g., due to new snowfall). An inverse distance weighting interpolation is finally used to create a regional map of the velocity results with 100 m grid spacing.

To establish errors associated with the speckle tracking technique, the mean velocity value was calculated over bedrock outcrops (i.e., areas with known zero motion) that surround each ice cap. From a total 3,816,019 points over bedrock, the mean error was < 6.5 m a^{-1}. This level error is within the margins reported by previous studies which utilize this method (Van Wychen et al. 2012), and well below the typical velocities of ~100-200 m a^{-1} observed at the terminus of ocean terminating glaciers.

3.2.2 Calculation of solid ice discharge

Two methods are used to determine ice discharge depending on the availability of ice thickness data. For glaciers where ice thickness data exists along a cross-section near the terminus, the flux through each section is calculated and then summed for the entire glacier width. To estimate ice discharge the change in velocity with depth through a glacier should also be known, but because this information is not directly available we assumed depth-averaged velocities between 80% and 100% of the surface velocity based on the work of Paterson (1994). For glaciers where only centreline measurements of ice thickness are available, we modelled the cross-sectional profile at the terminus. In this case, we assumed that the cross-sectional profile was between a 'V' and a 'U' shape. Our ice thickness data comes primarily from previous airborne radio-echo sounding measurements made by NASA (2012), Dowdeswell et al. (2004), Gogenini (1995) and Narod et al. (1988). Ice thicknesses on Axel Heiberg Island are derived using an area-depth scaling scheme completed by Ommanney (1969). The elapsed time between the acquisitions of the various measurement of ice thickness and the creation of velocity maps means that an error of 5 – 10 m is possible for the Dowdeswell et al. (2004) dataset, and higher additional error in the older datasets is possible.

3.3 Results and Discussion:

3.3.1 Surface ice velocities of the QEI

Surface ice velocities in the QEI are generally low on land-terminating glaciers (< 75 m a^{-1}) and higher on topographically constrained tidewater-terminating outlet glaciers (> 100 m a^{-1}). Ice velocities determined within the interior of each ice mass are generally < 10 m a^{-1}, which is indicative of ice that is frozen to its bed. In general, flow rates are similar to those suggested by earlier studies and closely match flow regimes in regions where they have previously been defined (e.g., Devon Ice Cap; Burgess et al. 2005).

3.3.2 Ice flux

Total ice discharge via calving from the QEI is estimated at 1.5 to 4.0 Gt a^{-1}. These values are similar to those estimated by Gardner et al. (2011) of 2.1 Gt a^{-1} to 4.9 Gt a^{-1} using an average mass loss per terminus width for glaciers with previously published velocity results. Prince of Wales Icefield is the largest contributor to mass loss via calving and ~50% of total ice loss is from just two glaciers: Trinity and Wykeham. Devon Ice Cap is the next largest contributor to mass loss via calving, with the majority of ice flux through the Belcher, Fitzroy and Southeast1 and Southeast2 glaciers. This estimate matches within error to the values estimated by Burgess et al. (2005) and Van Wychen et al. (2012). The Agassiz Ice Cap accounts for the next largest source of ice loss from iceberg calving, with estimates quite a bit lower than those proposed earlier by Williamson et al. (2008). This discrepancy may arise from the end of the surge of Eugenie Glacier as well as the use of winter velocities in this study, compared to summer velocities by Williamson et al. (2008). Table 3 summarizes the major contributors to the iceberg flux.

The other glaciers and ice caps in the QEI (Northern Ellesmere Ice Cap, Manson Icefield, Sydkap Ice Cap) are relatively minor contributors to iceberg fluxes at the present day (Table 3). However, the frequent occurrence of surge-type glaciers on these ice caps (Copland et al., 2003) suggests that iceberg discharges may vary by an order of magnitude or more between years. For example, Short and Gray (2005) determined that ice discharge from Otto Glacier (Northern Ellesmere Island) varied between 0.11 Gt a^{-1} in 2002, 0.37 Gt a^{-1} in 2003 and 0.61 Gt a^{-1} in 2004. Similarly, ice loss from Manson Icefield is likely to be highly variable due to the surge nature of

Mittie Glacier. Our results reveal ice velocities that are near stagnant at the terminus, but in 2003 velocities of ~1,000 m a^{-1} were observed at the calving front and as a result calving mass loss would have been greater at this time (Short and Gray 2005). As such, current calving rates from Manson Icefield are likely considerably less than what is possible from this ice mass.

Table 3. The ice caps and icefields of the QEI and their associated glaciers which contribute to the iceberg flux of the Canadian Arctic.

Ice cap/icefield	Glacier(s) contributing the majority of iceberg flux	Relative magnitude of iceberg flux contribution
Prince of Wales Icefield	Trinity & Wykeham	Major
Devon Ice Cap	Belcher, Fitzroy, Southeast1, Southeast2	Major
Agassiz Ice Cap		Major
Northern Ellesmere Ice Cap	Otto	Minor
Manson Icefield	Mittie	Minor
Sydkap Ice Cap		Minor

The presence of a large number of surging glaciers within the QEI which terminate into the ocean mean that calving mass loss is likely to be variable between years. However, due to the lack of knowledge with regard to the length of surge cycles for many glaciers within the QEI, future predictions of mass loss from the region are difficult. This necessitates the continual monitoring of surface velocities for the ice masses to produce year-to-year updates to iceberg production rates.

3.3.3 Conclusions

Speckle tracking of Radarsat-2 fine beam wide imagery was used to determine the surface velocity structure for all of the ice masses of the QEI. Results indicate that fast glacier flow (> 100 m a^{-1}) generally occurs on those that terminate in the ocean, while slower flow occurs on those terminate on land. Our ice velocity results compare well with those that have previously been determined, although they do reveal a year-to-year variation that is not necessarily a result of seasonal variation.

We estimate that total iceberg production from the QEI was approximately 1.5 - 4.0 Gt in 2012. These results are higher than previous estimates due to the inclusion of several glaciers which were omitted in previous studies. The majority of mass loss is discharged from the Trinity and Wykham glacier complex located in the southeastern region of Prince of Wales Icefield (Figure 7). The current lack of knowledge with regard to surge lengths and the number of surge glaciers within the QEI necessitates the continued monitoring of these glaciers to constrain iceberg production estimates in the future and to determine the variability in iceberg production between years.

4 General conclusions

The annual ice island and iceberg flux was estimated for ice shelf and tidewater glacier sources in the Canadian High Arctic (Table 4). These rates were quantified through analysis of satellite imagery and ice thickness data in GIS software. The ice island and iceberg flux into adjacent waters displayed large inter-annual variation, ranging from 1.6 to 13.3 Gt a^{-1}. This is due to the irregular nature of calving events and surge velocities of the respective ice shelves and glaciers of the QEI. Spatial augmentation of ice thickness data for full ice shelf extents and glacial termini, documentation of glacial surge lengths and an updated count of surge-type glaciers will improve the accuracy of flux calculations.

The ice island flux of the Ellesmere Island ice shelves, a known source of hazards for activity in the Western Canadian Arctic, was determined to be 1.8 Gt a^{-1} (1998 - 2012). The 2012 iceberg flux was estimated at approximately 1.5 – 4.0 Gt for CAA tidewater glaciers, with these icebergs primarily becoming hazards to Eastern Canadian Arctic operations.

Table 4. Summary of ice hazard fluxes: icebergs (IB) from the Queen Elizabeth Islands (QEI) and ice islands (II) from the Ellesmere Island (EI) ice shelves.

Region	Flux (Gt)	Flux record	Year/period
QEI	1.5 – 4.0	Total IB	2012
EI	20 ±3	Total II	1998 - 2012
EI	0	Minimum II	Observed in 5 separate years
EI	11 ±3.6	Maximum II	2008

Figure 8 illustrates the trajectories these ice hazards take after calving and where potential areas of concern are located due to overlapping ship trajectories. This research contributes information of use for the marine transportation industry on the production and occurrence of ice hazards. It is recommended that monitoring and analysis of calving events and glacial velocities continue, as both ice islands and icebergs pose serious risks to present and future offshore activity located within the Canadian Arctic.

References

Althoff WF (2007) Drift Station: Arctic Outposts of Superpower Science. Potomac Books Inc., Washington DC.

Barton R, Croasdale KR, Hnatiuk J, Smith JG (1972) Ice island count, southern Beaufort Sea 1972. Arct. Petrol. Opel. Assoc., Calgary, Alberta.

Belkin I, Kessel S (2013) Russian drifting stations on Arctic ice islands. In: Copland L, Mueller DR (eds) Arctic Ice Shelves and Ice Islands. Springer SBM, Dordrecht, In Press.

Burgess DO, Sharp MJ, Mair D, Dowdeswell, JA, Benham, TJ (2005) Flow dynamics and iceberg calving rates of Devon Ice Cap, Nunavut, Canada. J Glaciol, 51(173), 219–230. doi:10.3189/172756505781829430

Copland L (2009) Review of Recent Changes in Canadian Ice Shelves. University of Ottawa, Report prepared for Canadian Ice Service, 21 pp.

Copland L, Mueller DR, Weir L (2007) Rapid loss of the Ayles Ice Shelf, Ellesmere Island, Canada. Geophys Res Lett 34:L21501. doi:10.1029/2007GL031809.

Copland L, Sharp M, Dowdeswell J (2003) The distribution and flow characteristics of surge-type glaciers in the Canadian High Arctic. Annals of Glaciology, 36, 73-81.

Derksen C, Smith SL, Sharp M, Brown L, Howell S, Copland L, Mueller DR, Gauthier Y, Fletcher CG, Tivy A, Bernier M, Bourgeois J, Brown R, Burn CR, Duguay C, Kushner P, Langlois A, Lewkowicz AG, Royer A, Walker A (2012) Variability and change in the Canadian cryosphere. Clim Change 115:59–88. doi:10.1007/s10584-012-0470-0.

Dowdeswell, JA, Benham, T, Gorman, MR, Burgess, D, and Sharp, M (2004) Form and flow of the Devon Island Ice Cap, Canadian Arctic. J Geophys Res, 109(F2), 1–14. doi:10.1029/2003JF000095

Fletcher JO (1950) Floating ice islands in the Arctic Ocean. Tellus 2:323–324.

Gardner AS, Moholdt G, Wouters B, Wolken GJ, Burgess DO, Sharp MJ, Cogley JG (2011) Sharply increased mass loss from glaciers and ice caps in the Canadian Arctic Archipelago. Nature, 473(7347), 357–60. doi:10.1038/nature10089

Ghilani CD (2000) Demystifying area uncertainty: more or less. Surveying and Land Information Systems 60:177–182.

Gogenini P (1995) Remote sensing of polar ice [online]. Remote Sensing Laboratory, University of Kansas. Available: ftp://tornado.rsl.ukans.edu/pub/greenland/1995/pdf/may26_95.pdf

Hattersley-Smith G (1967) Note on ice shelves off the north coast of Ellesmere Island. Arc Circ 17:13–14.

Hattersley-Smith G, Crary AP, Christie RL (1955) Northern Ellesmere Island, 1953-1954. Arctic 8:3–36.

Hobson G (1989) Ice Island field station: New features of Canadian polar margin. EOS Trans Am Geophys Union 70:833, 835, 838–839.

Hochheim K, McCullough G, Babb D, Crawford A, Haogak C, Wolki J (2012) An integrated sea ice project for BREA (U of M): Detection, motion and RADARSAT mapping of extreme ice features in the southern Beaufort Sea. Field data report for the Beaufort Regional Environmental Assessment.

Jeffries MO (1982) The Ward Hunt Ice Shelf, Spring 1982. Arctic 35:542–544.

Jeffries MO (1986) Ice island calvings and ice shelf changes, Milne Ice Shelf and Ayles Ice Shelf, Ellesmere Island, N.W.T. Arctic 39:15–19.

Jeffries MO (1992) The source and calving of ice island ARLIS-II. Polar Rec 28:137–144.

Jeffries MO, Serson HV (1983) Recent changes at the front of Ward Hunt Ice Shelf, Ellesmere Island, N.W.T. Arctic 36:289–290.

Jeffries MO, Serson HV, Krouse HR, Sackinger WM (1991) Ice physical properties, structural characteristics and stratigraphy in Hobson's Choice Ice Island and implications for the growth history of East Ward Hunt Ice Shelf, Canadian High Arctic. J Glaciol 37:247–260.

Kealey C, Mueller D, Copland L (2011) Canadian Ice Shelves Breaking up at High Speed. Press Release, 27 September 2011.

Koenig LS, Greenaway KR, Dunbar M, Hattersley-Smith G (1952) Arctic ice islands. Arctic 5:68-95.

Mortimer CA, Copland L, Mueller DR (2012) Volume and area changes of the Milne Ice Shelf, Ellesmere Island, Nunavut, Canada, since 1950. J Geophys Res 117:F04011. doi:10.1029/2011JF002074.

Mortimer C (2011) Quantification of volume changes for the Milne Ice Shelf, Nunavut, 1950-2009. MSc Thesis, Department of Geography, University of Ottawa: Ottawa, Ontario.

Mueller DR, Copland L, Hamilton A, Stern DR (2008) Examining Arctic ice shelves prior to 2008 breakup. EOS Trans Am Geophys Union 89:502–503.

Mueller DR, Vincent WF, Jeffries MO (2003) Break-up of the largest Arctic ice shelf and associated loss of an epishelf lake. Geophys Res Lett 30:2031. doi:10.1029/2003GL017931.

Narod BB, Clarke, GKC, Prager BT (1988) Airborne UHF sounding of glaciers and ice shelves, northern Ellesmere Island, Arctic Canada, Can J Earth Sci, 25,95–105, doi:10.1139/e88-010.

Ommanney CSL (1969) The ice masses of Axel Heiberg Island, Canadian Arctic Archipelago: a study in glacier inventory. Axel Heiberg Island Research Reports, Glaciology no. 3, McGill University, Montreal, Quebec.

Peterson IK (2011) Ice island occurrence on the Canadian East Coast. Proc Intl Conf Port and Ocean Eng under Arctic Conditions. Held 10-14 July in Montréal, Canada. POAC11-044.

Pizzolato L, Howel S, Dawson J, Copland L, Derksen C, Johnston M (2013) *Climate Change Adaptation Assessment for Transportation in Arctic Waters (CATAW) Scoping Study*. A report prepared for Transport Canada. Ottawa, Ontario.

Pope S, Copland L, Mueller D (2012) Loss of multiyear landfast sea ice from Yelverton Bay, Ellesmere Island, Nunavut, Canada. Arct Antarct Alp Res 44:210–221.

Sharp M, Burgess DO, Cogley JG, Ecclestone M, Labine C, Wolken GJ (2011) Extreme melt on Canada's Arctic ice caps in the 21st century. Geophys Res Lett, 38(11), 3–7. doi:10.1029/2011GL047381

Spedding LG (1974) Ice island count, southern Beaufort Sea 1973. Arct. Petrol. Opel. Assoc., Calgary, Alberta.

Spedding LG (1977) Ice island count, southern Beaufort Sea 1976. Arct. Petrol. Opel. Assoc., Calgary, Alberta.

Stephenson SR, Smith LC, Brigham LW, and Agnew JW (2013) Projected 21st-century changes to Arctic marine access. Climatic Change. DOI:10.1007/s10584-D12-0685-D.

Taylor JR (1997) An introduction to error analysis: The study of uncertainties in physical measurements. University Science Books.

Van Wychen W, Copland L., Gray L, Burgess D, Danielson B, Sharp M (2012) Spatial and temporal variation of ice motion and ice flux from Devon Ice Cap, Nunavut, Canada. J Glaciol, 58(210), 657–664. doi:10.3189/2012JoG11J164

Vincent WF, Gibson JAE, Jeffries MO (2001) Ice shelf collapse, climate change, and habitat loss in the Canadian high Arctic. Polar Rec 37:133–142.

White A (2012) Dynamics and historical changes of the Petersen ice shelf and epishelf lake, Nunavut, Canada, since 1959. MSc Thesis, Department of Geography, University of Ottawa: Ottawa, Ontario.

Williamson S, Shar, M, Dowdeswell J, Benham, T (2008) Iceberg calving rates from northern Ellesmere Island ice caps, Canadian Arctic, 1999 – 2003. J Glaciol, 54(186), 391–400.

Figures

Figure 1. Examples of: (a) an ice island from the Ward Hunt Ice Shelf, Ellesmere Island (2008), (b) an iceberg adrift in Baffin Bay (2013), and (c & d) damage caused to ship hulls due to iceberg collisions. Photos courtesy of: (a) Sam Soja, (b) Anna Crawford, and (c & d) the Canadian Ice Service, Environment Canada.

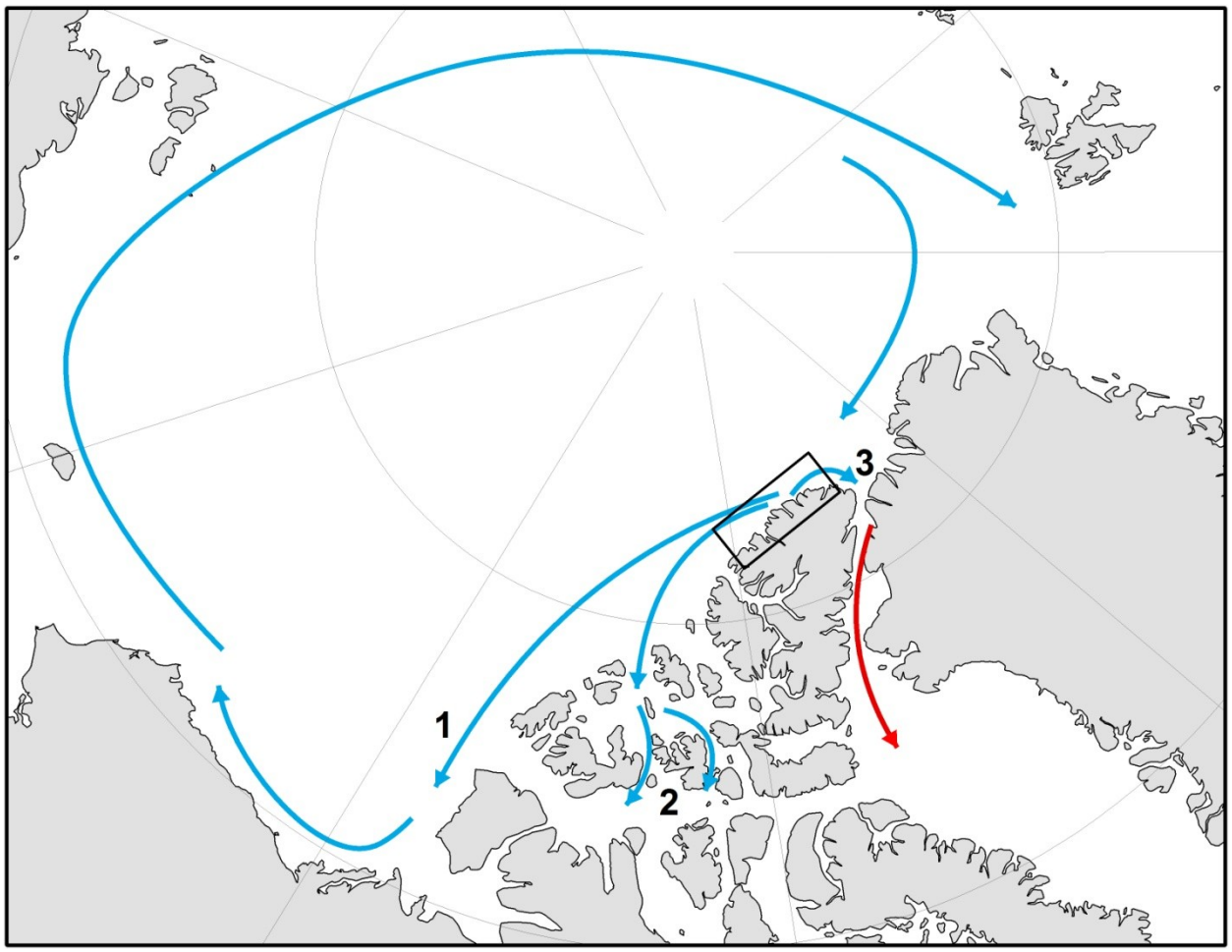

Figure 2. Map of the Arctic Ocean showing the region where thick ice shelves are found along the northern coast of Ellesmere Island (black rectangle). Generalized drift tracks from these ice islands are indicated in blue. The most common historically has been a clockwise circulation in the Beaufort Gyre (1). However, it is also possible for drift through the Canadian Arctic Archipelago (2) to occur when sea ice cover is light. Ice islands rarely travel south via Kennedy Channel (3). Other ice islands are produced by the calving floating glacier tongues of northwestern Greenland, such as Petermann Gletscher. These ice islands drift south along the coast of Baffin Island (red arrow).

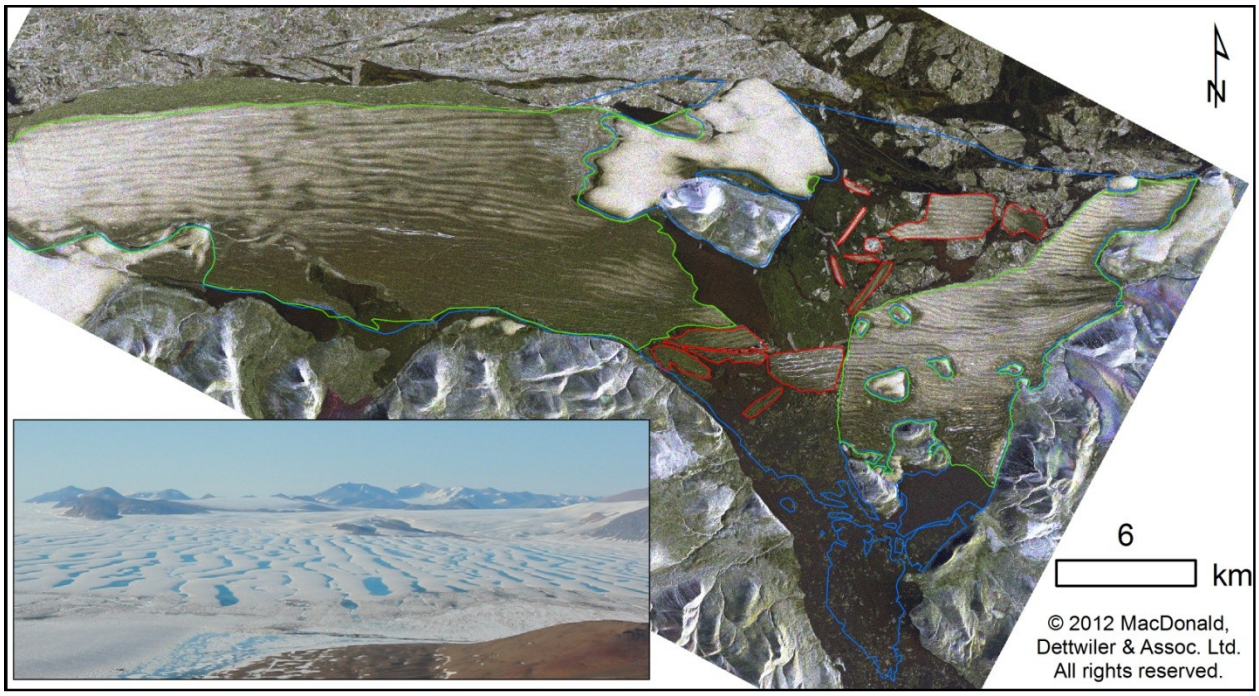

Figure 3. A fine quad-polarimetric mode Radarsat-2 image of the Ward Hunt Ice Shelf in April 2012. The extent of the ice shelf is delineated in green, detached ice islands are shown in red and the extent of the ice shelf in 2000 is outlined in blue. The ridge and trough morphology that characterizes Canadian Arctic ice shelves and ice islands is visible in both the satellite image and the inset photograph of the eastern portion of the ice shelf. The photograph was taken from Ward Hunt Island in the centre of the ice shelf in 2003 before extensive ice break-up began.

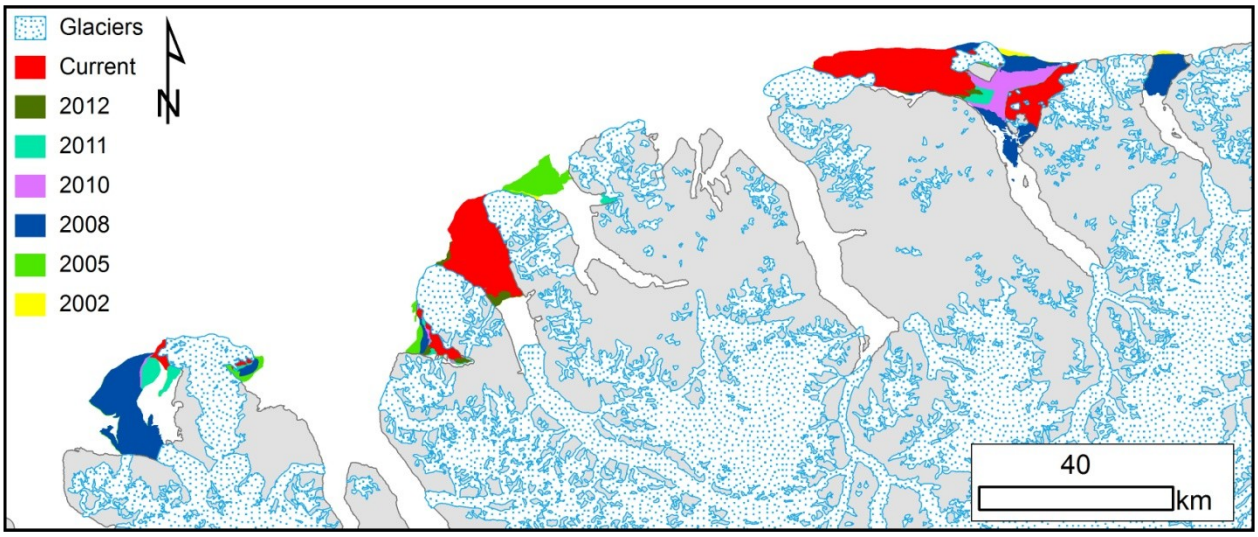

Figure 4. The extent of ice shelves along the northern coast of Ellesmere Island. The current extent is shown in red and the extent of loss over the study period is indicated by the colour in the legend. The extent of the ice shelves at the beginning of the study period is indicated by all the colours combined.

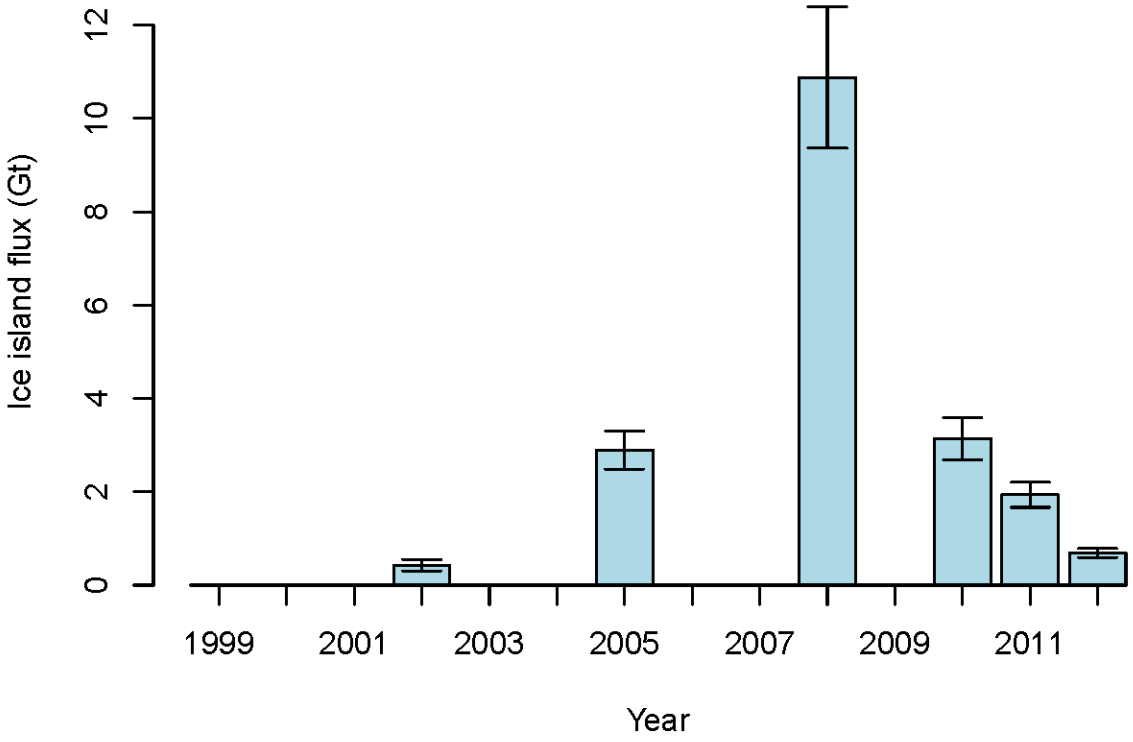

Figure 5. Ice island flux in billions of metric tons of ice per year from the Canadian Arctic ice shelves over the last 15 years.

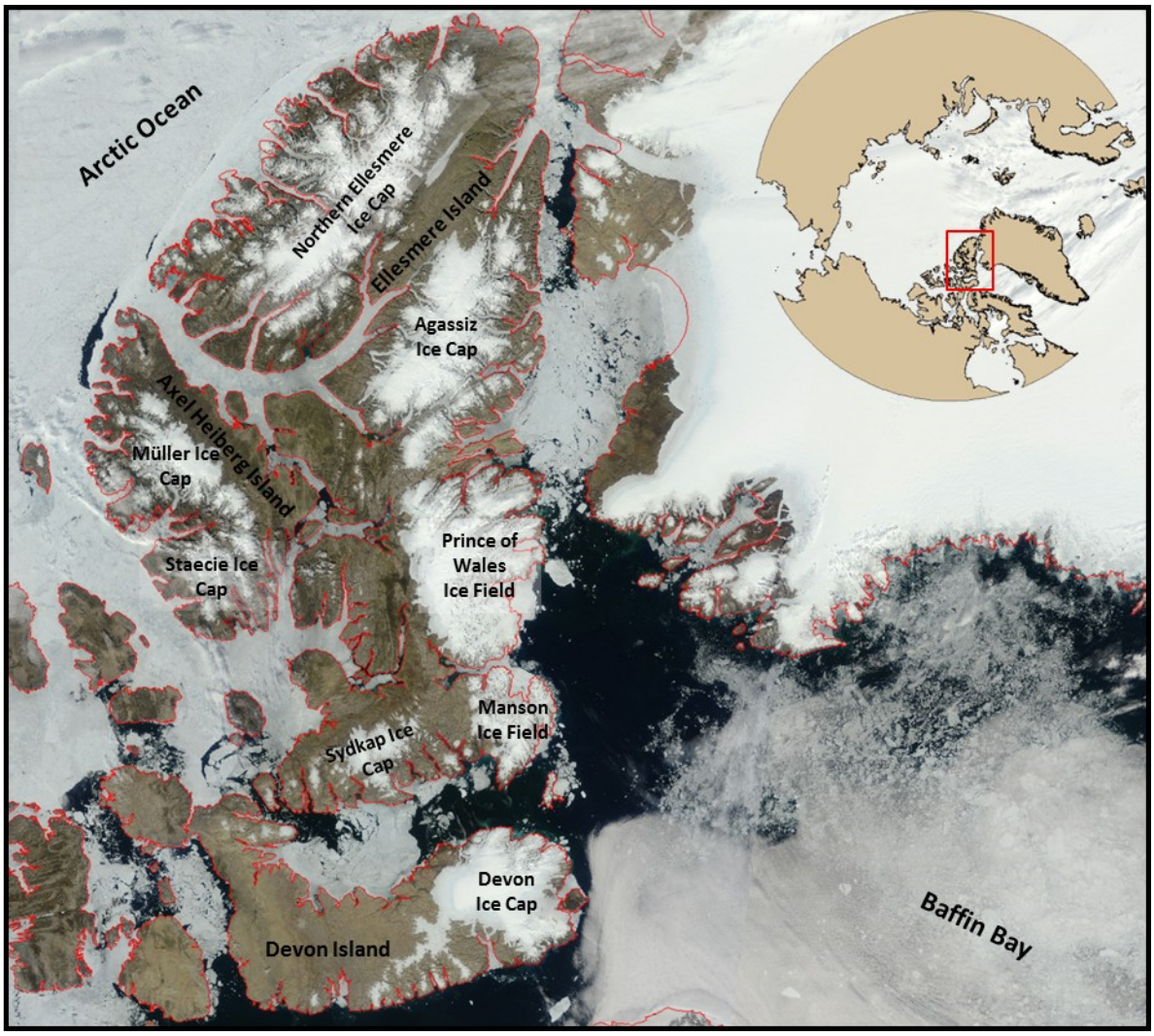

Figure 6. Study area: location of glaciers and ice caps in the Queen Elizabeth Islands (QEI), Nunavut.

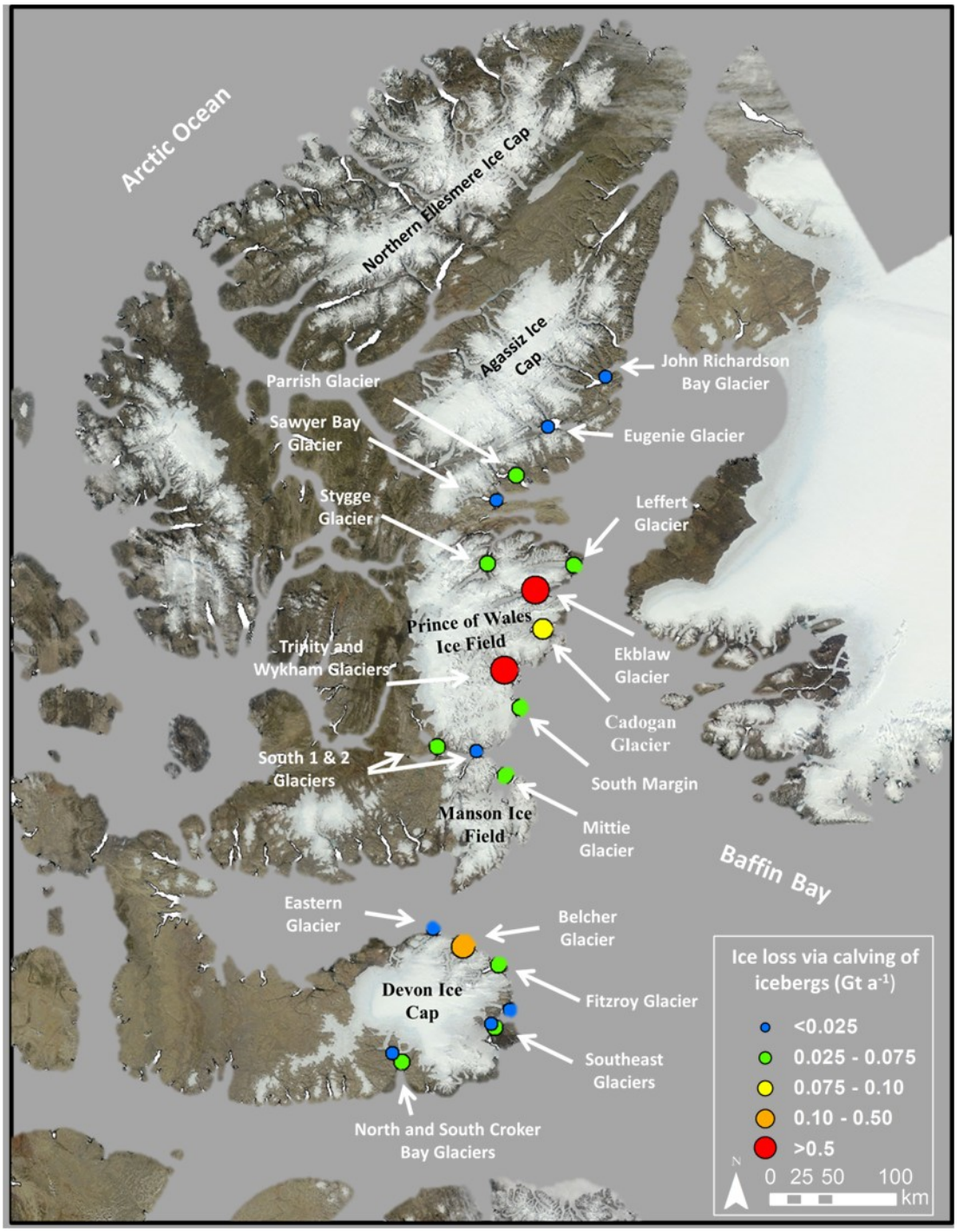

Figure 7. Primary locations of iceberg production in the Queen Elizabeth Islands (QEI) for 2012 (rates in gigatons per year; 1 gigaton = 1,000,000,000 tons of ice).

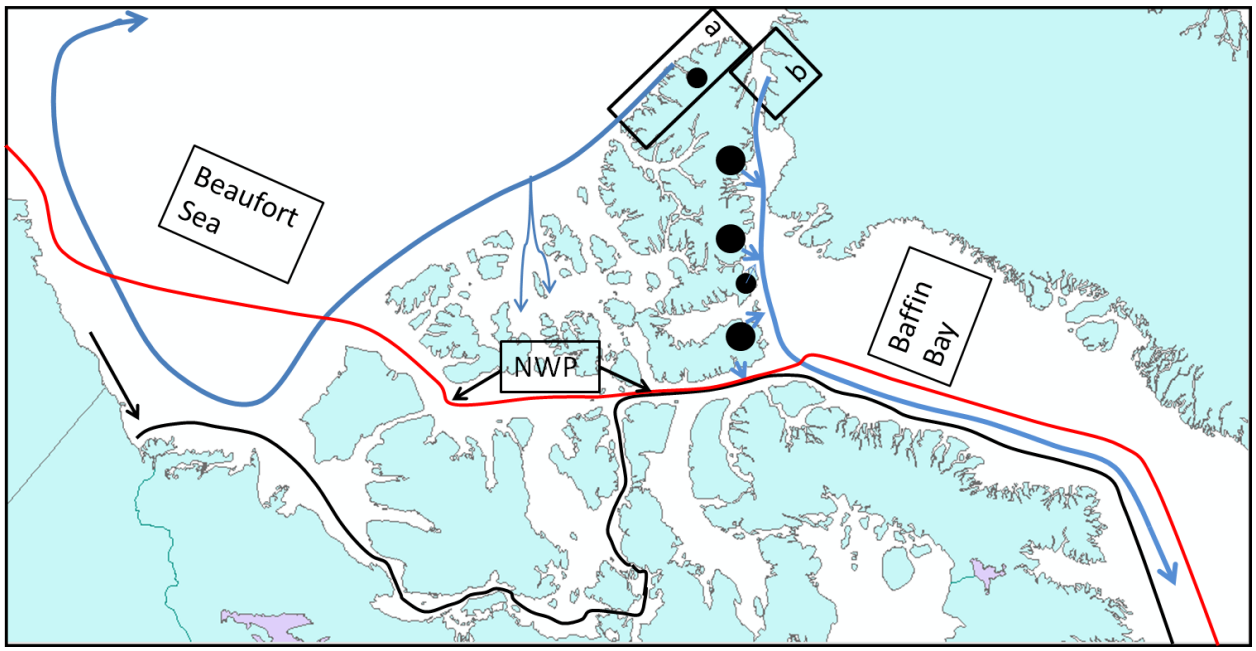

Figure 8. Ice hazard (blue) and ship (red & black) trajectories in the Canadian Arctic. Regions with potential collision danger include the Beaufort Sea, Northwest Passage (NWP) and Baffin Bay. Ice hazards include ice islands sourced from the Ellesmere Island ice shelves (a) and the Petermann Gletscher (b) as well as icebergs sourced from the tidewater glaciers of the (north to south) Ellesmere Island, Agassiz, Prince of Wales, Manson and Devon ice caps/icefields (black circles). Circles are weighted to depict the respective magnitude of iceberg flux (not to scale). Ship trajectories include the NWP route (red) from Stephenson et al. (2013) and Northern Transportation System and Northern Projects Management proposed routes (black), courtesy of Transport Canada.

Appendix A

Imagery used to determine ice shelf extents and derive iceberg fluxes.

Table A-1. Imagery used to determine ice shelf extents. Supplemental imagery (Optical: MODIS, ASTER, Formosat-2; and other SAR imagery) were used between the images below to ensure the accuracy of the timing of events and to provide context and complementary information for ice type identification.

Acquisition date	Satellite	Beam Mode	Resolution (m)
1998-01-13	Radarsat-1	ScanSAR-Wide	100
2003-01-07	Radarsat-1	Standard Beam	27
2003-01-11	Radarsat-1	ScanSAR-Wide	100
2006-01-13	Radarsat-1	Standard Beam	27
2006-01-14	Radarsat-1	Standard Beam	27
2006-01-15	Radarsat-1	Standard Beam	27
2006-01-16	Radarsat-1	Standard Beam	27
2009-01-04	Radarsat-2	ScanSAR-Wide	160
2011-02-28	Radarsat-2	Fine Beam	10
2011-03-19	Radarsat-2	Fine Beam	10
2011-03-23	Radarsat-2	Fine Beam	10
2011-04-25	Radarsat-2	Ultrafine Beam	3
2012-02-03	Radarsat-2	Ultrafine Beam	3
2012-02-08	Radarsat-2	Ultrafine Beam	3
2012-04-18	Radarsat-2	Fine Quad Beam	8
2012-08-24	Radarsat-2	Fine Quad Beam	8
2012-08-24	Radarsat-2	Fine Quad Beam	8
2012-08-24	Radarsat-2	Fine Quad Beam	8
2012-08-24	Radarsat-2	Fine Quad Beam	8
2012-08-27	Radarsat-2	Fine Quad Beam	8

Table A-2. Summary of satellite data used to derive iceberg fluxes.

Ice Mass	Acquisition Dates (2012)	Beam Mode	Polarization	Scenes
Prince of Wales Icefield	Apr 9 - May 3	Fine Wide (9m)	HH	2
Agassiz Ice Cap	Mar 16 – Apr 9	Fine Wide (9m)	HH	2
	Jan 12 – Feb 5	Fine Wide (9m)	HH	1
Northern Ellesmere Ice Cap	Jan 28 – Feb 21	Fine Wide (9m)	HH	3
	Jan 27 – Feb 20	Fine Wide (9m)	HH	2
Müller & Stacie Ice Caps	Feb 27 – Mar 22	Fine Wide (9m)	HH	2
Sydkap Ice Cap	Jan 12 – Feb 5	Fine Wide (9m)	HH	1
Manson Icefield	Apr 9 - May 3	Fine Wide (9m)	HH	1
Devon Ice Cap	Apr 9 – May 3	Fine Wide (9m)	HH	1
	Feb 7 – Mar 2	Ultrafine Wide (3m)	HH	1
	Jan 31 – Feb 24	Ultrafine Wide (3m)	HH	1